

## Supplemental Data

### Ca<sup>2+</sup> Requirements for Cerebellar

#### Long-Term Synaptic Depression:

#### Role for a Postsynaptic Leaky Integrator

Keiko Tanaka, Leonard Khiroug, Fidel Santamaria, Tomokazu Doi,

Hideaki Ogasawara, Graham Ellis-Davies, Mitsuo Kawato,

and George J. Augustine

#### Coincidence of Ca<sup>2+</sup> with PF activity induces LTD

When coupled with PF stimulation, the rise in [Ca<sup>2+</sup>]<sub>i</sub> resulting from CF activity can cause LTD (Sakurai, 1990; Konnerth et al., 1992). We asked whether the elevation of [Ca<sup>2+</sup>]<sub>i</sub> by uncaging DMNPE-4 could substitute for CF activity to induce LTD, as previously observed with a different caged Ca<sup>2+</sup> compound by Lev-Ram et al. (1997).

At the frequency and intensity employed in our experiments, PF stimulation alone did not elevate [Ca<sup>2+</sup>]<sub>i</sub> measurably (Figure S1A, left) and was incapable of inducing LTD (Figure S1B). (More robust PF activity can elevate [Ca<sup>2+</sup>]<sub>i</sub> and produce LTD: Eilers et al., 1995; Hartell, 1996; Eilers et al., 1997.) Likewise, uncaging DMNPE-4 with a 1 Hz train of UV light pulses for 30 s (6.5 μJ per pulse, 195 μJ total), which produced transient increases in [Ca<sup>2+</sup>]<sub>i</sub> similar to those described in Figure 2 (Figure S1A, middle), was not sufficient to depress PF synaptic transmission in the experiment shown in Figure S1B. However,

activating PF synapses while elevating  $[Ca^{2+}]_i$ , by uncaging DMNPE-4, caused a gradual decline in the amplitude of PF-EPSCs. This depression of PF synaptic transmission reached a new steady level that was 47% of control EPSC amplitude in the example shown in Figure S1B. During the pairing of PF activity with uncaged  $Ca^{2+}$ , the peak level of  $[Ca^{2+}]_i$  measured during the UV light pulses was very similar to that produced by the UV light pulses alone (Figure S1A, right). But the activity of PF synapses caused baseline  $[Ca^{2+}]_i$  to rise more rapidly (red lines in Figure S1A). This may be due to a synergistic action of uncaged  $Ca^{2+}$  and the IP3 that is produced by PF activity (Finch and Augustine, 1998; Takechi et al., 1998) upon IP3 receptors (Iino, 1990; Bezprozvanny et al., 1991; Finch et al., 1991).

We performed 3 experiments where PF activity was paired with  $[Ca^{2+}]_i$  elevation. In each case, LTD was induced and the mean level of depression was  $49 \pm 3\%$  of the initial control PF-EPSC amplitude. These reductions in PF synaptic response occurred without any changes in pipette series resistance, or in the input resistance and holding current of the Purkinje cell, indicating that they reflect changes in PF synaptic efficacy rather than a recording artifact. The depression had an exponential time course, with a time constant of  $4.9 \pm 0.5$  min. The magnitude and kinetics of the LTD produced by pairing PF activity with  $[Ca^{2+}]_i$  elevation were comparable to those observed when LTD is induced by combining PF activity with CF activity or Purkinje cell depolarization (Konnerth et al., 1992; Karachot et al., 1994; Leitges et al., 2004). These results demonstrate that  $[Ca^{2+}]_i$  elevation and PF activity can act synergistically to induce LTD.

### **Ca<sup>2+</sup>-induced LTD shares signaling pathways with conventional LTD**

It is known that LTD results from the clathrin-dependent internalization of postsynaptic AMPA receptors (Wang and Linden, 2000). To determine whether Ca<sup>2+</sup>-induced LTD is due to the same mechanism, we asked whether a peptide inhibitor of clathrin assembly prevents the LTD induced by repetitive uncaging of Ca<sup>2+</sup>. This peptide, termed AP2pep, acts by preventing assembly of clathrin into membrane coats (Morgan et al., 2000). When AP2pep was introduced into Purkinje cells through the patch pipette, increasing [Ca<sup>2+</sup>]<sub>i</sub> caused little or no LTD (Figure S2A, open symbols). On average, PF-EPECs were reduced by only 2.8±2.7% following DMNPE-4 photolysis in the presence of AP2pep (n=6). As a control, we also examined the action of a mutant peptide, AP2ΔDLL peptide, which has a disrupted clathrin binding site and is less able to inhibit assembly of clathrin (Morgan et al., 2000). In the presence of AP2ΔDLL, Ca<sup>2+</sup>-induced LTD was still observed (Figure S2A, filled symbols). The reduction in PF-EPSC amplitude produced by uncaging Ca<sup>2+</sup> was 27.1±2.7% (n=4) in the presence of AP2ΔDLL, which is significantly larger (p<0.001) than the amount of LTD observed in the presence of AP2pep. However, AP2ΔDLL did reduce the amount of LTD somewhat, perhaps due to the reported weak ability of AP2 ΔDLL peptide to block clathrin assembly at high concentrations (Morgan et al., 2000). The preferential ability of AP2pep to prevent Ca<sup>2+</sup>-induced LTD indicates that this form of LTD depends on clathrin-dependent membrane traffic, as is the case for conventional LTD induced by synaptic activity.

In its magnitude and time course, as well as its requirements for  $\text{Ca}^{2+}$  and for clathrin-dependent membrane trafficking,  $\text{Ca}^{2+}$ -induced LTD resembles the LTD induced by pairing PF synaptic activity with CF activity and/or depolarization. To determine the relationship between these two forms of LTD more directly, we asked whether they share the same downstream signaling pathway. Specifically, we asked whether induction of one form of LTD prevents any further depression of synaptic transmission by the other form of LTD. This type of occlusion experiment frequently has been used to determine whether forms of hippocampal synaptic plasticity share common pathways (Gustafsson et al., 1987; Kauer et al., 1988; Muller et al., 1990; Cormier et al., 1993; Oliet et al., 1997).

In our experiments, stimuli that evoked  $\text{Ca}^{2+}$ -induced LTD and synaptically-evoked LTD were sequentially presented to single Purkinje cells. When LTD was first elicited by pairing PF activity with depolarization of the Purkinje cell membrane potential ( $\Delta V_{\text{PF}}$  in Figure S2B), subsequent elevation of  $[\text{Ca}^{2+}]_i$  via DMNPE-4 photolysis ( $\text{Ca}$  in the Figure S2B) produced no further depression of PF-EPSCs (upper part of Figure S2B;  $n=3$ ). The average reduction in PF-EPSC amplitude caused by pairing PF activity with depolarization was  $44 \pm 3\%$ , while PF-EPSCs were reduced subsequently by only  $4 \pm 5\%$  following  $[\text{Ca}^{2+}]_i$  elevation ( $n=3$ ). Likewise, initially inducing LTD by elevating  $[\text{Ca}^{2+}]_i$  prevented any further depression of PF-EPSC amplitude by later pairing of PF activity with depolarization (lower part of Figure S2B;  $n=3$ ). On average,  $[\text{Ca}^{2+}]_i$  elevation reduced PF-EPSCs by  $55 \pm 1\%$ , while subsequent paired stimulation reduced PF-EPSCs by only  $5 \pm 3\%$  ( $n=3$ ). In summary, induction of one form of

LTD prevented subsequent induction of the other form. This mutual occlusion indicates that LTD and  $\text{Ca}^{2+}$ -induced LTD share a final common signaling pathway.

### **Spatial range of $\text{Ca}^{2+}$ -induced LTD**

LTD induced by pairing localized PF synaptic activity with depolarization spreads approximately 50  $\mu\text{m}$  beyond active PF synapses to neighboring PF synapses (Wang et al., 2000; Reynolds and Hartell, 2000). Similar observations have been made for LTD induced by high amounts of PF activity alone (Hartell, 1996; Eilers et al., 1997). Because the signals responsible for such spread of LTD are not clear, we next asked whether the LTD induced by local elevation of  $[\text{Ca}^{2+}]_i$  was capable of spreading.

Our first approach to this question involved locally stimulating two beams of PF axons: one at the site of  $\text{Ca}^{2+}$  uncaging, which monitored the induction of LTD at this site, and another at variable distances away from the site of  $[\text{Ca}^{2+}]_i$  elevation. Figure S3A illustrates an experiment where two stimulating pipettes were placed 43  $\mu\text{m}$  apart to activate two non-overlapping PF beams. Previous work has established that such stimuli activate PF synapses within an area approximately 5  $\mu\text{m}$  in radius from the position of the pipette (Wang et al., 2000). A train of UV light pulses (1 Hz, 30 s) was applied only at the location of the first stimulation pipette. During the time that  $\text{Ca}^{2+}$  was photoreleased, neither set of PFs were activated; after  $[\text{Ca}^{2+}]_i$  returned to the resting level, PF stimulation was resumed at both sites. With this protocol, only the PF synapses at the first PF

input underwent LTD, while transmission at the second PF input remained unchanged (Figure S3A). This result indicates that LTD induced by local elevation of  $[Ca^{2+}]_i$  does not spread as far as LTD induced by synaptic activation.

To more precisely determine the spatial range of LTD induction, we performed a second set of experiments where the UV spot was positioned at a variable distance from a single site of PF activation. Data from 24 such experiments are summarized in Figure S3B, where the degree of depression of PF-EPSC amplitude is plotted as a function of the separation between the PF stimulating electrode and the site of  $[Ca^{2+}]_i$  elevation. Again, it is apparent that the LTD induced by  $[Ca^{2+}]_i$  elevation is restricted in its spread. These data could be described by a Gaussian function with a half-width of  $10.2 \pm 1.5 \mu\text{m}$  (solid line in Figure S3B). This value is virtually identical to the dimensions of the region of  $[Ca^{2+}]_i$  elevation (Figure 1), indicating that LTD induced by local elevation of  $[Ca^{2+}]_i$  does not spread beyond locations where  $[Ca^{2+}]_i$  is elevated.

### **Lack of LTD following repeated subthreshold rises in $[Ca^{2+}]_i$**

Experiments such as the one illustrated in Figure 3A and 3B show that elevating  $[Ca^{2+}]_i$  to different levels three times causes LTD only after the third UV light pulse, which raised  $[Ca^{2+}]_i$  to the highest level. One interpretation of this result is that  $[Ca^{2+}]_i$  must exceed a threshold level to induce LTD. However, a reviewer suggested that this depression might be due to the fact that the third light pulse was preceded by two prior pulses of UV light, which could have damaged the Purkinje cell sufficiently to depress PF transmission. To determine whether

depression was due to suprathreshold  $[Ca^{2+}]_i$  elevation, or to repeated illumination, we applied two UV light pulses (200  $\mu$ J) that caused subthreshold rises in  $[Ca^{2+}]_i$  (Figure S4A) and monitored PF-EPSC (Figure S4B). While both the first and second pulses elevated  $[Ca^{2+}]_i$  to 0.8  $\mu$ M, PF-EPSC amplitude remained unchanged. This indicates that subthreshold elevation of  $[Ca^{2+}]_i$  was incapable of inducing LTD even though UV light was applied twice. Thus, we conclude that the depression occurring in Figure 3B after the third light pulse is due to  $[Ca^{2+}]_i$  exceeding the threshold level, thereby inducing LTD.

#### **“Leaky integrator” description of LTD**

We propose that  $[Ca^{2+}]_i$  is integrated to produce a downstream signal, termed X. X could correspond to any number of elements in the signal transduction pathway downstream of  $Ca^{2+}$ , such as one or more activated proteins (e.g., protein kinase C, PKC) or other signals. If integrated  $Ca^{2+}$  exceeds some threshold, then LTD occurs in an all-or-none manner. The integration of  $[Ca^{2+}]_i$  is not perfect but is associated with some leak. Production of X can then be described by the following differential equation:

$$\tau \frac{dx}{dt} = -x + a[Ca^{2+}]_i(t) \quad (S1)$$

where  $x$  denotes the concentration of the signal X,  $\tau$  is the time constant of the leaky integrator, and  $a$  represents the efficiency of converting  $[Ca^{2+}]_i$  to  $x$ .

In our experiments, a prolonged pulse of UV light produced a ramp-like rise in  $[Ca^{2+}]_i$ . In this case, the time-dependent rise in  $[Ca^{2+}]_i$  can be described as:

$$[Ca^{2+}]_i(t) = kt \quad (S2)$$

where  $k$  is the slope of  $[Ca^{2+}]_i$  increase. Substituting Eqn. (S2) into Eq. (S1) yields:

$$\tau \frac{dx}{dt} = -x + akt \quad (S3)$$

With an initial condition of  $[Ca^{2+}]_i = 0$ , the solution of Eqn. (S3) is:

$$x(t) = ak\tau \exp\left(-\frac{t}{\tau}\right) + ak(t - \tau) \quad (S4)$$

Because we do not know the level of  $x$  required to produce LTD, we assume that LTD is produced when  $x$  reaches a threshold level. At saturating  $[Ca^{2+}]_i$ , the maximum amount of LTD is a 36% reduction in PF-EPSC amplitude, irrespective of the duration of  $[Ca^{2+}]_i$  elevation (Figure 5C). We therefore assumed that the threshold value of  $x$  is reached when LTD is half of the maximum, that is an 18% reduction in PF-EPSCs. This amount of LTD is achieved when  $[Ca^{2+}]_i = K_{Ca}$ , so that the threshold ( $\theta$ ) is:

$$\theta = a\left(\frac{K_{Ca}}{t}\right)\tau \exp\left(-\frac{t}{\tau}\right) + a\left(\frac{K_{Ca}}{t}\right)(t - \tau) \quad (S5)$$

We used this relationship to determine the values of  $a$  and  $\tau$  that best described the dependence of  $K_{Ca}$  on the duration of  $[Ca^{2+}]_i$  elevation (Figure 5B). For this purpose,  $a$  and  $\tau$  were varied and eqn. S5 was used to determine the resulting value of  $K_{Ca}$ . The error in the derived value of  $K_{Ca}$ , defined as the sum of squares difference between the solution of eqn. S5 and the data points shown in Figure 5B, is shown for a range of values of  $a$  and  $\tau$  in Figure S5A. The minimum error occurred at a single point (red peak in Figure S5A) when  $a = 18.7$  and  $\tau = 0.56$ . These values provided a good description of the duration-dependence of  $K_{Ca}$ , as

can be seen from the smooth curve in Figure S5B and the comparison to the experimental data shown in Figure 5B. Further, because  $[Ca^{2+}]_i$  was elevated in a ramp-like fashion, where the integral of  $[Ca^{2+}]_i$  is one-half the product of  $[Ca^{2+}]_i$  and the duration of the UV light pulse,  $K_{Ca-integ}$  values could also be predicted from the following relationship:

$$\theta = a \left( \frac{2K_{Ca-integ}}{t^2} \right) \tau \exp\left(-\frac{t}{\tau}\right) + a \left( \frac{2K_{Ca-integ}}{t^2} \right) (t - \tau) \quad (S6)$$

As shown by the line in Figure S5C, the predicted values showed a duration-dependence that emulated the relationship observed in the experimental measurements (Figure 6B).

If LTD occurs when  $x$  reaches a threshold level, the relationship between LTD and  $x$  should be independent of the duration of the  $Ca^{2+}$  signal that generated  $x$ . To assess this, we plotted the amount of LTD, measured experimentally for different durations of  $[Ca^{2+}]_i$  elevation, as a function of  $x$  produced by a given rise in peak  $[Ca^{2+}]_i$ . The relative value of  $x$  was determined from the following relationship, obtained by combining eqn. S2 and eqn. S4:

$$x = a \left( \frac{[Ca^{2+}]_i}{t} \right) \tau \exp\left(-\frac{t}{\tau}\right) + a \left( \frac{[Ca^{2+}]_i}{t} \right) (t - \tau) \quad (S7)$$

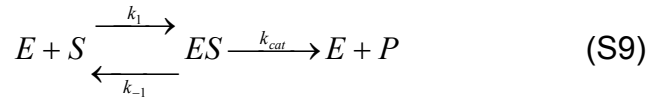
The relationship between LTD and the relative value of  $x$  was indeed found to be independent of duration (Figure 6E), providing support for our conclusion that the dynamic behavior of LTD arises from a leaky integrator.

## Positive feedback loop model

The Kuroda et al. (2001) mathematical model of signal transduction pathways for cerebellar LTD was used to simulate the relationship between  $\text{Ca}^{2+}$  and LTD. As a measure of LTD, we used the calculated percentage of phosphorylated AMPA receptors at 100 min after increasing  $[\text{Ca}^{2+}]_i$ . This model (Figure 7A) included the biochemical and enzymatic reactions shown in Figure S6. Reversible biochemical reactions can be described by the following formula:



where  $k_f$  and  $k_b$  are the forward and backward rate constants. Enzymatic reactions were defined from the standard Michaelis-Menten scheme:



In this formula, enzyme E first binds to its substrate S and then catalyzes a reaction that produces P.  $k_1$  and  $k_{-1}$  are the forward and backward rate constants for the binding reaction, and  $k_{cat}$  is the rate constant for the catalytic reaction. The values used for each of these reaction kinetic parameters are listed in Table S1 and the concentrations of each reactant are listed in Table S2. These values were determined based on the previous reports indicated in the right-most columns of Tables S1 and S2.

Because the present study focuses on LTD triggered by  $\text{Ca}^{2+}$ , we used only the part of the Kuroda et al. (2001) model that is downstream of  $\text{Ca}^{2+}$ . This model is available on-line (<http://www.cns.atr.jp/neuroinfo/>). To take into account the conditions of our  $\text{Ca}^{2+}$  uncaging experiments and recent insights into signal

transduction reactions, the following two modifications were first made: (1) In the original model, the activity of phosphatase (PP2A) was decreased in response to synaptic activity. In our experiments, synapses were not activated during LTD induction; for this reason, the concentration of active PP2A was assumed to be constant at 0.045  $\mu\text{M}$ . (2) In the original model, PKC was assumed to be degraded after activation, thus resulting in deactivation of the positive feedback loop. Because there is no evidence for such a PKC degradation reaction, this step was eliminated from the present version of the model and the degradation rate of arachidonic acid (AA) was increased from 0.001 to 0.4/s, as was done in another study (Bhalla and Iyengar, 1999). Two other small modifications were necessary to accurately reproduce our experimental results: (3) To obtain the correct value for  $K_{\text{Ca}}$ , the  $\text{Ca}^{2+}$  dissociation constant of PKC was reduced from 10 to 2  $\mu\text{M}$ . The Hill coefficient for activation of PKC by  $\text{Ca}^{2+}$  also was increased from 1 to 2, to reflect the actual number of  $\text{Ca}^{2+}$  ions that bind to a single PKC molecule (Sutton and Sprang, 1998; Verdaguer et al., 1999). (4) After the modifications described above, the model predicted that almost 100% of the AMPA receptors would be phosphorylated, so that the amplitude of PF-EPSCs would be reduced to zero. To obtain a percentage of LTD similar to what was observed experimentally (~36%), the rate of phosphorylation of AMPA receptors by PKC was reduced to 0.05/s.

We examined how varying these values or concentrations affects the  $\text{Ca}^{2+}$  triggering of LTD by repeating the simulation while systematically varying each of the 64 parameters. These parameters included the time constant of biochemical

reactions ( $\tau$ ),  $k_{cat}$ ,  $K_d$ ,  $K_{eq}$ , or  $K_m$  in reactions shown in Table S1 (a1-d2) and the concentrations of molecules shown in Table S2. For each parameter, we varied the values over a 10,000-fold range, using 6 values lower than the original values (1/100, 2/100, 5/100, 1/10, 2/10, and 5/10 of the original value) and 6 higher values (2, 5, 10, 20, 50, or 100 times the original value). In total, we collected 768 relationships between  $[Ca^{2+}]_i$  and LTD, all based on elevating  $[Ca^{2+}]_i$  for 1 s.

A graphic representation of the outcome of this exploration of parameter space is shown in Figure S7. This figure illustrates the influence of changing each parameter, indicated at the bottom of the figure, on several aspects of the predicted relationship between  $[Ca^{2+}]_i$  and LTD, such as the  $K_{Ca}$  value (Figure S7A), maximum amount of LTD (Figure S7B), and Hill coefficient (Figure S7C). In many cases, depression occurred even in the absence of elevated  $[Ca^{2+}]_i$ ; such effects were quantified by determining the basal amount of depression at 0  $\mu M$   $[Ca^{2+}]_i$  (Figure S7D). In these plots, the dashed horizontal lines indicate the outcome produced by the parameter values used in the final model, while the colored symbols indicate results obtained when the parameters were set to other values. In 175 out of the 768 relationships, basal depression was 10% or more and the sigmoidal  $Ca^{2+}$ -dependence of LTD was absent. We therefore fit the Hill equation to the remaining 593 relationships. Varying parameters had little or no effect on  $K_{Ca}$  in 72% of the cases and on the maximum amount of LTD in 51% of the cases. In contrast, the Hill coefficient was very parameter-sensitive, so that the Hill coefficient was unchanged in only 16% of the 593 relationships. The spatial gradients in  $[Ca^{2+}]_i$  and the noise associated with experimental

measurements were not considered here, so that the Hill coefficient was very large (dashed line). In fact, in our deterministic simulation, the Hill coefficient theoretically should become infinitely large because of the bistable dynamics of the system, as indicated in Figure 7B. The finite values of Hill coefficient observed were due to finite intervals between simulated points and/or to poor fits of the Hill equation. We believe that Hill coefficients of 5 or greater for a given parameter set indicates that the system is highly cooperative and bistable. From this point of view, the high cooperativity property was preserved in 53% of the 593 relationships.

To quantify the parameter-sensitivity of these predictions, we calculated the standard deviations (SD) of  $K_{Ca}$ , maximum LTD, and Hill coefficient values obtained when each parameter was varied over the 10,000-fold range (Table S3 and S4). In addition to describing the robustness of the simulation, these analyses reveal some biologically interesting trends. In particular, the simulation was particularly sensitive to the parameters that control  $Ca^{2+}$ -dependent activation of PKC - such as the reactions included in Figure S6A and PKC concentration - as well as the parameters that regulate AMPA receptor phosphorylation. These results suggest that the reactions which determine PKC activity or AMPA receptor phosphorylation are biochemical control points that may be precisely regulated at synapses to control LTD induction.

The nonlinear and bistable nature of the model, which is evident as the all-or-none behavior shown in Figure 7B, was greatly affected by variations in parameter values. To quantify such effects, we calculated the difference (max-

basal) between the maximal (at 10  $\mu\text{M}$   $[\text{Ca}^{2+}]_i$ ) and basal (Figure S7D) values for LTD, as shown in Figure S7E. For the case of Figure 7B, max-basal was 35% and this value is indicated by the dotted line in Figure S7E. In most cases, bistability was associated with max-basal values of 30% or more. Variations in reactions d1 and d2 were exceptional, because they yielded bistability independent of the max-basal values. As shown in Figure S7E, bistability was particularly sensitive to variations in parameters related to activation of mitogen-activated protein kinase (MAPK, b reactions). The loss of bistability in these reactions was also associated with a low Hill coefficient (Figure S7C), consistent with our conclusion that cooperativity requires the positive feedback loop. Because MAPK is in the positive feedback loop, these results are consistent with our conclusion that bistability arises from this loop. Further, these results suggest that regulating MAPK activity may be a control point for regulating the positive feedback loop and LTD induction.

### **Refining the simulation by taking into account experimental conditions**

The simulation described above is not spatially resolved, meaning that it considers a situation where  $[\text{Ca}^{2+}]_i$  (and indeed all components of the signaling cascade) is spatially homogeneous. While such a situation is appropriate for considering LTD at the level of single synapses, it does not fully replicate the conditions of our experiments, where the Gaussian distribution of UV light produced a similar gradient in  $[\text{Ca}^{2+}]_i$  (Figure 1).

To take into account this gradient of  $[Ca^{2+}]_i$ , we described the spatial profile (S) of  $[Ca^{2+}]_i$  with a Gaussian function (equation S10):

$$S(a_k, w_j, x_i) = (a_k + w_j) e^{-x_i^2 / 2\sigma_{uv}^2} \quad (S10)$$

where  $a_k$  is the maximum amplitude of the uncaged  $Ca^{2+}$  and  $x_i$  is the distance from the center of the uncaging spot. We incorporated a homegenously distributed random variable ( $w_j$ ) to introduce a noise term comparable to the fluctuations in laser intensity and  $Ca^{2+}$  uncaging efficiency over time during illumination. The maximum amplitude,  $a_k$ , was varied from 0 to 10  $\mu$ M, the range of  $[Ca^{2+}]_i$  covered by the simulation. Our experimental measurements (eg. Figure 1) show that  $\sigma_{uv} = 5 \mu$ m and suggest that the range of values for  $w_j$  is close to 25% of the maximum amplitude.

In addition to spatial variations in  $[Ca^{2+}]_i$ , it is also necessary to take into account reductions in the number of active PFs with increasing distance from the stimulating electrode. This is necessary because any effect of elevated  $[Ca^{2+}]_i$  that is outside of the area of activated PF synapses will not be reported in our measurements of LTD, which are based on responses of activated PF synapses. Therefore, we used equation S10 to calculate the spatially averaged value of S over the dendritic region occupied by activated PFs. The measurements of Wang et al. (2000) indicated that this area has a radius,  $r$ , of 3  $\mu$ m. In all of our experiments we were careful to align the stimulating electrode with the center of the uncaging spot, so the two Gaussian functions were concentric.

$$S_x(a_k, w_j) = \frac{1}{2r} \sum_{x_i=-r}^{x_i=r} S(a_k, w_j, x_i) \quad (S11)$$

We then used the Hill equation to determine the values of LTD produced at each point within this area of active PFs:

$$LTD(a_k, w_j) = \frac{S_x(a_k, w_j)^n}{K_{Ca}^n + S_x(a_k, w_j)^n} \quad (S12)$$

where  $K_{Ca}$  and  $n$  are the values for  $[Ca^{2+}]_i$  required for half-maximal LTD and the Hill coefficient, respectively. Both  $K_{Ca}$  and  $n$  were extracted from fitting the Hill equation to the simulation results shown in Figure 7B. Finally, because our measurements of LTD were integrated over all activated PF synapses, we estimated the average value of LTD produced by a given  $a_k$ . This was done by taking into account laser power fluctuations and changes in uncaging efficiency by taking  $N = 50$  samples of the randomly distributed variable  $w$ .

$$\overline{LTD}(a_k) = \frac{1}{N} \sum_{w_j=w_1}^{w_j=w_N} \frac{S(a_k, w_j)^n}{K_{Ca}^n + S(a_k, w_j)^n} \quad (S13)$$

This average LTD calculation yielded a very good approximation of the experimental measurements of the  $[Ca^{2+}]_i$  dependence of LTD, as shown in Figure 7C. This concordance between the modeling results and experimental measurements suggest that LTD is an all-or-none event at the single spine level that is blurred in experimental measurements due to spatial variations in  $[Ca^{2+}]_i$  and to noise.

## Supplemental References

- Ahn, S., Ginty, D. D., and Linden, D. J. (1999). A late phase of cerebellar long-term depression requires activation of CaMKIV and CREB. *Neuron* 23, 559-568.
- Bezprozvanny, I., Watras, J., and Ehrlich, B. E. (1991). Bell-shaped calcium-response curves of Ins(1,4,5)P<sub>3</sub>- and calcium-gated channels from endoplasmic reticulum of cerebellum. *Nature* 351, 751-754.
- Bhalla, U. S., and Iyengar, R. (1999). Emergent properties of networks of biological signaling pathways. *Science* 283, 381-387.
- Channon, J. Y., and Leslie, C. C. (1990). A calcium-dependent mechanism for associating a soluble arachidonoyl-hydrolyzing phospholipase A<sub>2</sub> with membrane in the macrophage cell line RAW 264.7. *J. Biol. Chem.* 265, 5409-5413.
- Charles, C. H., Abler, A. S., and Lau, L. F. (1992). cDNA sequence of a growth factor-inducible immediate early gene and characterization of its encoded protein. *Oncogene* 7, 187-190.
- Charles, C. H., Sun, H., Lau, L. F., and Tonks, N. K. (1993). The growth factor-inducible immediate-early gene 3CH134 encodes a protein-tyrosine-phosphatase. *Proc. Natl. Acad. Sci. USA* 90, 5292-5296.
- Chen, S. J., Klann, E., Gower, M. C., Powell, C. M., Sessoms, J. S., and Sweatt, J. D. (1993). Studies with synthetic peptide substrates derived from the neuronal protein neurogranin reveal structural determinants of potency and selectivity for protein kinase C. *Biochemistry* 32, 1032-1039.

- Cormier, R. J., Mauk, M. D., and Kelly, P. T. (1993). Glutamate iontophoresis induces long-term potentiation in the absence of evoked presynaptic activity. *Neuron* 10, 907-919.
- Eilers, J., Callewaert, G., Armstrong, C., and Konnerth, A. (1995). Calcium signaling in a narrow somatic submembrane shell during synaptic activity in cerebellar Purkinje neurons. *Proc. Natl. Acad. Sci. USA* 92, 10272-10276.
- Eilers, J., Takechi, H., Finch, E. A., Augustine, G. J., and Konnerth, A. (1997). Local dendritic  $Ca^{2+}$  signaling induces cerebellar long-term depression. *Learn. Mem.* 4, 159-168.
- Finch, E. A., and Augustine, G. J. (1998). Local calcium signalling by inositol-1,4,5-trisphosphate in Purkinje cell dendrites. *Nature* 396, 753-756.
- Finch, E. A., Turner, T. J., and Goldin, S. M. (1991). Calcium as a coagonist of inositol 1,4,5-trisphosphate-induced calcium release. *Science* 252, 443-446.
- Force, T., Bonventre, J. V., Heidecker, G., Rapp, U., Avruch, J., and Kyriakis, J. M. (1994). Enzymatic characteristics of the c-Raf-1 protein kinase. *Proc. Natl. Acad. Sci. USA* 91, 1270-1274.
- Gustafsson, B., Wigström, H., Abraham, W. C., and Huang, Y. Y. (1987). Long-term potentiation in the hippocampus using depolarizing current pulses as the conditioning stimulus to single volley synaptic potentials. *J. Neurosci.* 7, 774-780.
- Hartell, N. A. (1996). Strong activation of parallel fibers produces localized calcium transients and a form of LTD that spreads to distant synapses. *Neuron* 16, 601-610.

- Haystead, T. A., Dent, P., Wu, J., Haystead, C. M., and Sturgill, T. W. (1992). Ordered phosphorylation of p42mapk by MAP kinase kinase. *FEBS Lett.* *306*, 17-22.
- Huang, C. Y., and Ferrell, J. E., Jr. (1996). Ultrasensitivity in the mitogen-activated protein kinase cascade. *Proc. Natl. Acad. Sci. USA* *93*, 10078-10083.
- lino, M. (1990). Biphasic  $Ca^{2+}$  dependence of inositol 1,4,5-trisphosphate-induced Ca release in smooth muscle cells of the guinea pig taenia caeci. *J. Gen. Physiol.* *95*, 1103-1122.
- Karachot, L., Kado, R. T., and Ito, M. (1994). Stimulus parameters for induction of long-term depression in in vitro rat Purkinje cells. *Neurosci. Res.* *21*, 161-168.
- Kauer, J. A., Malenka, R. C., and Nicoll, R. A. (1988). NMDA application potentiates synaptic transmission in the hippocampus. *Nature* *334*, 250-252.
- Konnerth, A., Dreessen, J., and Augustine, G. J. (1992). Brief dendritic calcium signals initiate long-lasting synaptic depression in cerebellar Purkinje cells. *Proc. Natl. Acad. Sci. USA* *89*, 7051-7055.
- Kuroda, S., Schweighofer, N., and Kawato, M. (2001). Exploration of signal transduction pathways in cerebellar long-term depression by kinetic simulation. *J. Neurosci.* *21*, 5693-5702.
- Kyriakis, J. M., App, H., Zhang, X. F., Banerjee, P., Brautigan, D. L., Rapp, U. R., and Avruch, J. (1992). Raf-1 activates MAP kinase-kinase. *Nature* *358*, 417-421.

- Leitges, M., Kovac, J., Plomann, M., and Linden, D. J. (2004). A unique PDZ ligand in PKC $\alpha$  confers induction of cerebellar long-term synaptic depression. *Neuron* *44*, 585-594.
- Leslie, C. C., and Channon, J. Y. (1990). Anionic phospholipids stimulate an arachidonoyl-hydrolyzing phospholipase A2 from macrophages and reduce the calcium requirement for activity. *Biochim. Biophys. Acta* *1045*, 261-270.
- Lev-Ram, V., Jiang, T., Wood, J., Lawrence, D. S., and Tsien, R. Y. (1997). Synergies and coincidence requirements between NO, cGMP, and Ca<sup>2+</sup> in the induction of cerebellar long-term depression. *Neuron* *18*, 1025-1038.
- Marquez, C., Martinez, C., Kroemer, G., and Bosca, L. (1992). Protein kinase C isoenzymes display differential affinity for phorbol esters. Analysis of phorbol ester receptors in B cell differentiation. *J. Immunol.* *149*, 2560-2568.
- Morgan, J. R., Prasad, K., Hao, W., Augustine, G. J., and Lafer, E. M. (2000). A conserved clathrin assembly motif essential for synaptic vesicle endocytosis. *J. Neurosci.* *20*, 8667-8676.
- Muller, D., Buchs, P. A., Dunant, Y., and Lynch, G. (1990). Protein kinase C activity is not responsible for the expression of long-term potentiation in hippocampus. *Proc. Natl. Acad. Sci. USA* *87*, 4073-4077.
- Mumby, M. C., Green, D. D., and Russell, K. L. (1985). Structural characterization of cardiac protein phosphatase with a monoclonal antibody. Evidence that the Mr = 38,000 phosphatase is the catalytic subunit of the native enzyme(s). *J. Biol. Chem.* *260*, 13763-13770.

- Nemenoff, R. A., Winitz, S., Qian, N. X., Van Putten, V., Johnson, G. L., and Heasley, L. E. (1993). Phosphorylation and activation of a high molecular weight form of phospholipase A2 by p42 microtubule-associated protein 2 kinase and protein kinase C. *J. Biol. Chem.* 268, 1960-1964.
- Oancea, E., and Meyer, T. (1998). Protein kinase C as a molecular machine for decoding calcium and diacylglycerol signals. *Cell* 95, 307-318.
- Oliet, S. H., Malenka, R. C., and Nicoll, R. A. (1997). Two distinct forms of long-term depression coexist in CA1 hippocampal pyramidal cells. *Neuron* 18, 969-982.
- Pato, M. D., Sutherland, C., Winder, S. J., and Walsh, M. P. (1993). Smooth-muscle caldesmon phosphatase is SMP-I, a type 2A protein phosphatase. *Biochem. J.* 293, 35-41.
- Reynolds, T., and Hartell, N. A. (2000). An evaluation of the synapse specificity of long-term depression induced in rat cerebellar slices. *J. Physiol.* 527, 563-577.
- Sakurai, M. (1990). Calcium is an intracellular mediator of the climbing fiber in induction of cerebellar long-term depression. *Proc. Natl. Acad. Sci. USA* 87, 3383-3385.
- Sanghera, J. S., Paddon, H. B., Bader, S. A., and Pelech, S. L. (1990). Purification and characterization of a maturation-activated myelin basic protein kinase from sea star oocytes. *J. Biol. Chem.* 265, 52-57.

- Schaechter, J. D., and Benowitz, L. I. (1993). Activation of protein kinase C by arachidonic acid selectively enhances the phosphorylation of GAP-43 in nerve terminal membranes. *J. Neurosci.* 13, 4361-4371.
- Seger, R., Ahn, N. G., Posada, J., Munar, E. S., Jensen, A. M., Cooper, J. A., Cobb, M. H., and Krebs, E. G. (1992). Purification and characterization of mitogen-activated protein kinase activator(s) from epidermal growth factor-stimulated A431 cells. *J. Biol. Chem.* 267, 14373-14381.
- Storm, S. M., Cleveland, J. L., and Rapp, U. R. (1990). Expression of raf family proto-oncogenes in normal mouse tissues. *Oncogene* 5, 345-351.
- Sun, H., Charles, C. H., Lau, L. F., and Tonks, N. K. (1993). MKP-1 (3CH134), an immediate early gene product, is a dual specificity phosphatase that dephosphorylates MAP kinase in vivo. *Cell* 75, 487-493.
- Sutton, R. B., and Sprang, S. R. (1998). Structure of the protein kinase C beta phospholipid-binding C2 domain complexed with  $Ca^{2+}$ . *Structure* 6, 1395-1405.
- Takechi, H., Eilers, J., and Konnerth, A. (1998). A new class of synaptic response involving calcium release in dendritic spines. *Nature* 396, 757-760.
- Tanaka, J., Matsuzaki, M., Tarusawa, E., Momiyama, A., Molnar, E., Kasai, H., and Shigemoto, R. (2005). Number and density of AMPA receptors in single synapses in immature cerebellum. *J. Neurosci.* 25, 799-807.
- Verdaguer, N., Corbalán-García, S., Ochoa, W. F., Fita, I., and Gómez-Fernández, J. C. (1999).  $Ca^{2+}$  bridges the C2 membrane-binding domain of

protein kinase Calpha directly to phosphatidylserine. *EMBO J* 18, 6329-6338.

Wang, S. S., Khiroug, L., and Augustine, G. J. (2000). Quantification of spread of cerebellar long-term depression with chemical two-photon uncaging of glutamate. *Proc. Natl. Acad. Sci. USA* 97, 8635-8640.

Wang, Y. T., and Linden, D. J. (2000). Expression of cerebellar long-term depression requires postsynaptic clathrin-mediated endocytosis. *Neuron* 25, 635-647.

Wijkander, J., and Sundler, R. (1991). An 100-kDa arachidonate-mobilizing phospholipase A2 in mouse spleen and the macrophage cell line J774. Purification, substrate interaction and phosphorylation by protein kinase C. *Eur. J. Biochem.* 202, 873-880.

## Supplementary Figures

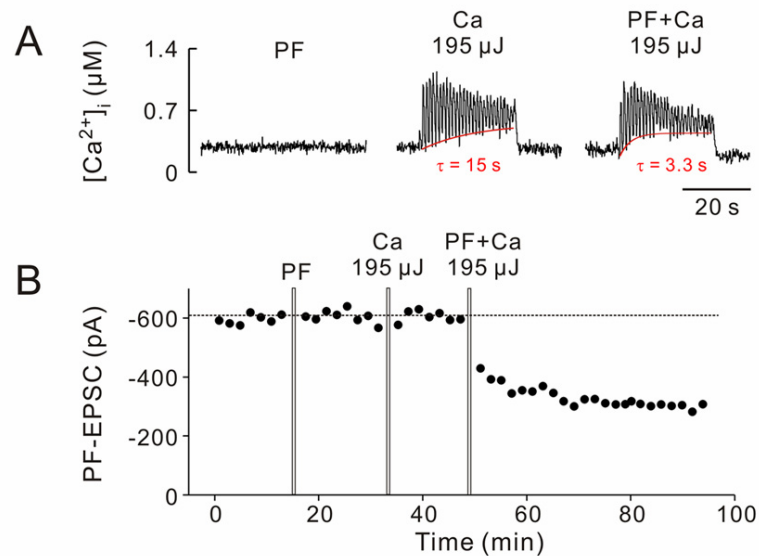


Figure S1

LTD is induced by pairing of PF activation and  $Ca^{2+}$  uncaging

(A) Time course of  $[Ca^{2+}]_i$  increase evoked in the same cell by each of the three trains. Note lack of  $[Ca^{2+}]_i$  increase in response to PF stimulation alone. The exponential fitting curves for the baseline  $Ca^{2+}$  during a train of pulse are shown by red line and the tau for uncaging  $Ca^{2+}$  alone and for pairing PF stimulation with uncaging  $Ca^{2+}$  is 15 and 3.3 s, respectively. (B) PF-EPSC amplitude (circles) is at a stable level (dashed line) prior to and after the 30 s 1 Hz train of PF stimuli (vertical bar, PF) and after the  $Ca^{2+}$  uncaging train (Ca). However, when the two stimuli are paired (PF+Ca), a rapid, LTD-like decrease in EPSC amplitude occurs.

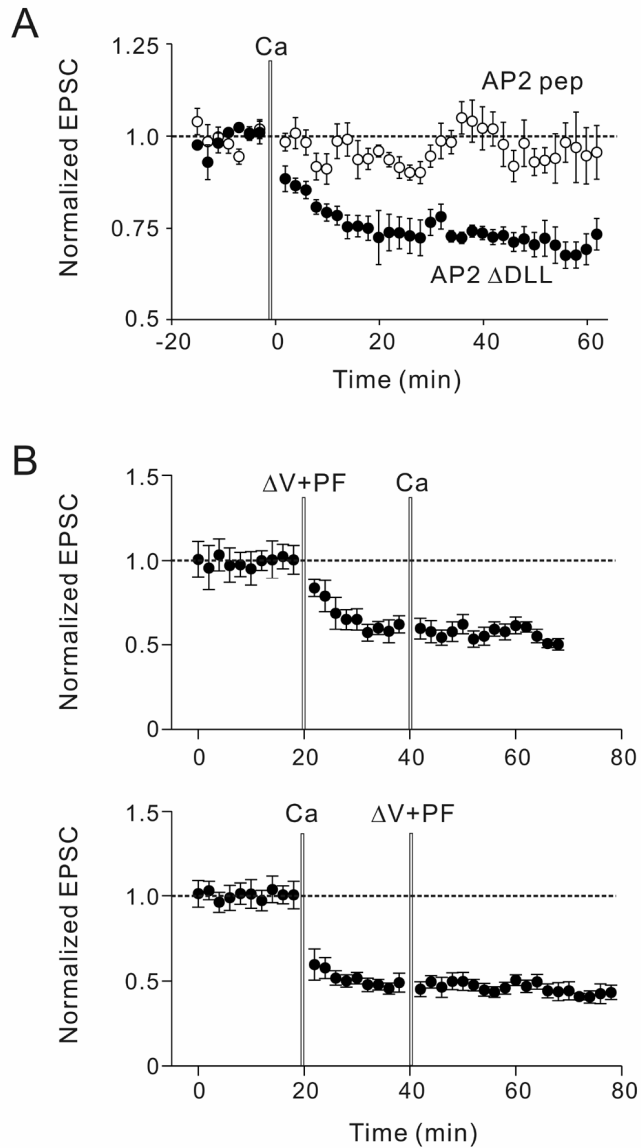


Figure S2

### Intracellular signaling pathways of Ca<sup>2+</sup>-induced LTD

(A) Ca<sup>2+</sup>-induced LTD is dependent on clathrin-mediated endocytosis. When a control AP2 peptide (AP2  $\Delta$ DLL, 1.56 mM) was applied intracellularly (filled circles), PF-EPSC amplitude undergoes LTD after 1 Hz train of Ca<sup>2+</sup> uncaging (vertical bar; Ca). In contrast, when AP2 peptide was applied intracellularly

(open circles),  $\text{Ca}^{2+}$ -induced LTD was blocked. Current amplitudes are normalized to the mean of pre-train level for each cell (dashed line). Data are shown as mean  $\pm$  SEM from 4 experiments for each peptide. (B)  $\text{Ca}^{2+}$ -induced LTD and conventional LTD mutually occlude each other. Upper panel: Averaged normalized PF-EPSC amplitude undergoes LTD upon a 30 s 1 Hz train of depolarizing steps (to 0 mV for 100 ms) paired with PF stimuli. Twenty minutes later, when LTD has reached its maximal level, a similar train of  $\text{Ca}^{2+}$  uncaging fails to cause further depression of PF-EPSC amplitude. Dashed line indicates the pre-treatment level to which current amplitude is normalized. Lower panel: After LTD is induced by a train of  $\text{Ca}^{2+}$  uncaging, pairing of depolarization with PF stimulation did not produce any change in PF-EPSC amplitude.

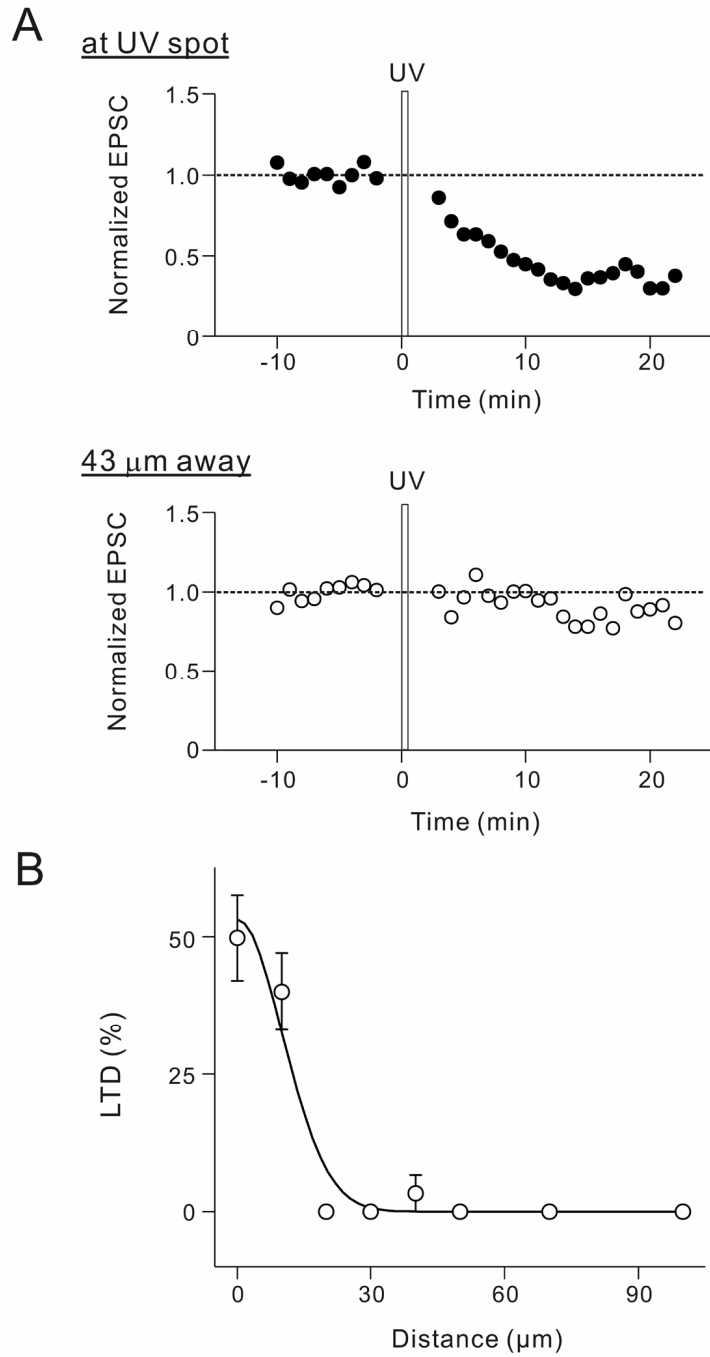


Figure S3

Spatial range of  $\text{Ca}^{2+}$ -induced LTD

(A) An example of experiment with two stimulation pipettes activating two separate inputs 43  $\mu\text{m}$  apart. A train of  $\text{Ca}^{2+}$  uncaging produces LTD of the first

input (at UV spot) but causes no change on the second input (43  $\mu\text{m}$  away). (B) Pooled data from the experiments with varied distance between the activated PF synapses and the uncaging spot. The amount of depression upon a  $\text{Ca}^{2+}$  uncaging train which would normally cause LTD, is plotted as a function of the distance. The smooth line is a Gaussian function.

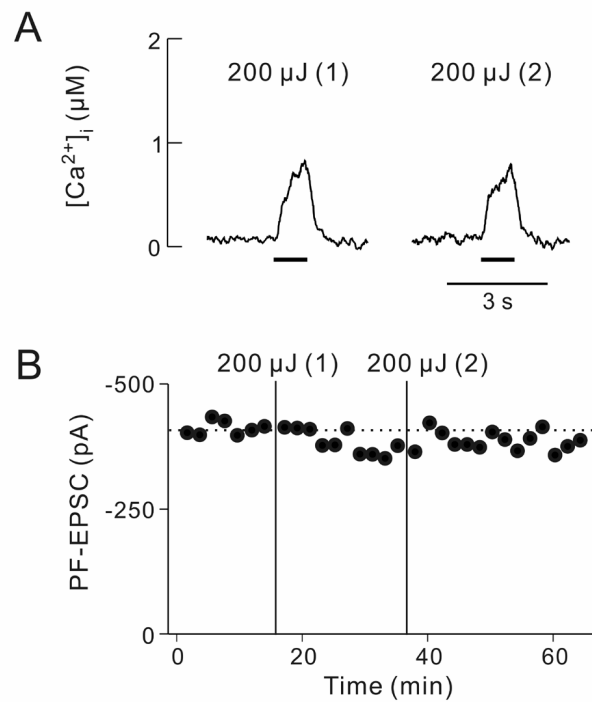


Figure S4

LTD is not induced by subthreshold level of rise in  $[Ca^{2+}]_i$  applied twice in a single Purkinje cell.

(A) Time course of  $[Ca^{2+}]_i$  increases evoked in a Purkinje cell by two UV pulses (horizontal bars) of same intensities. (B) Time course of PF-EPSC amplitude. No depression was observed after either first (1) or second (2) increase in  $[Ca^{2+}]_i$  shown in A.

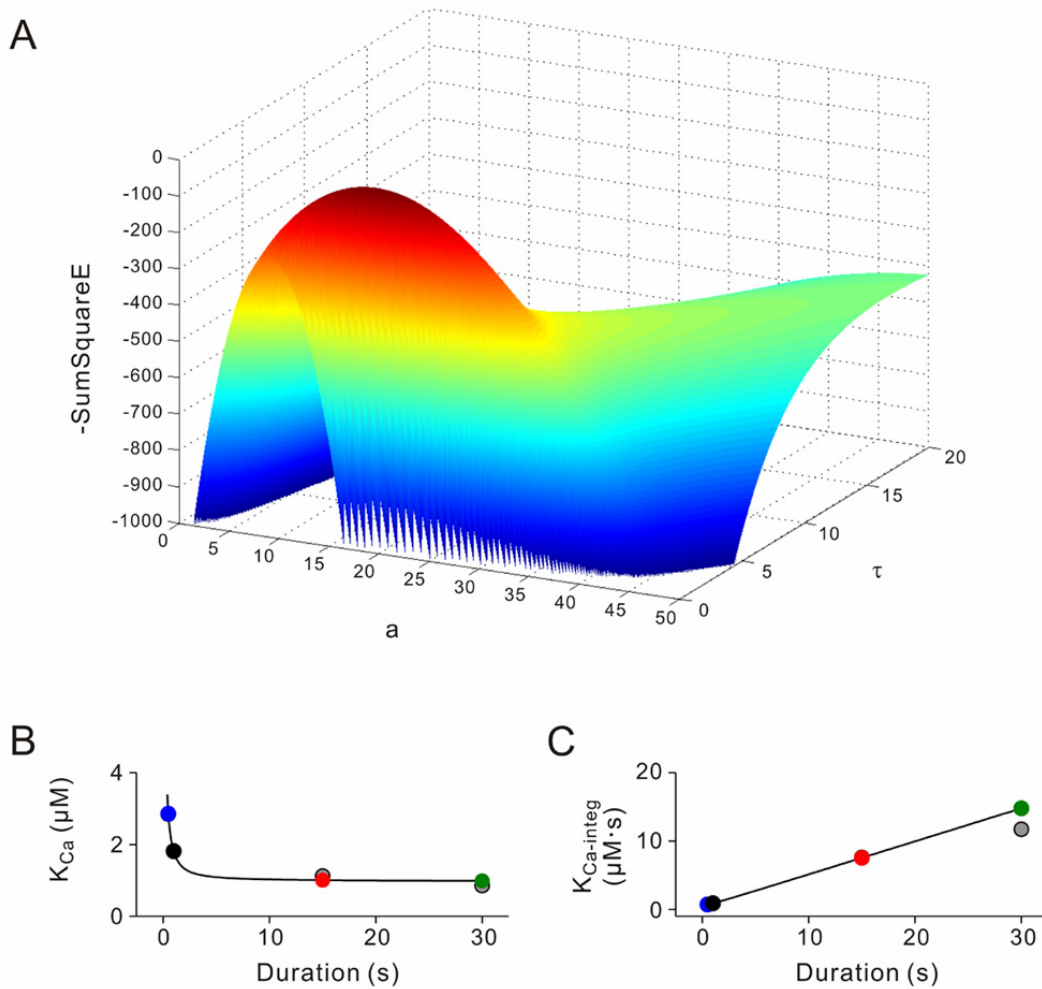


Figure S5

(A) Plot of the error of the theoretically predicted  $K_{Ca}$  values for experimental data points from Figure 5B as a function of the two parameter values;  $a$  and  $\tau$ . The error is defined as the sum of squared difference of the theoretical prediction and data points. The landscape has a unique local maxima, corresponding to minimum prediction error, at  $a=18.7$  and  $\tau=0.56$ . (B and C) The theoretically predicted  $K_{Ca}$  values (B) and  $K_{Ca-area}$  values (C) are plotted against duration of  $[\text{Ca}^{2+}]_i$  elevation. These values were calculated from eqn. S5 and S6. For comparison, experimental data shown in Figures 5B and 6B are also plotted as gray circles.



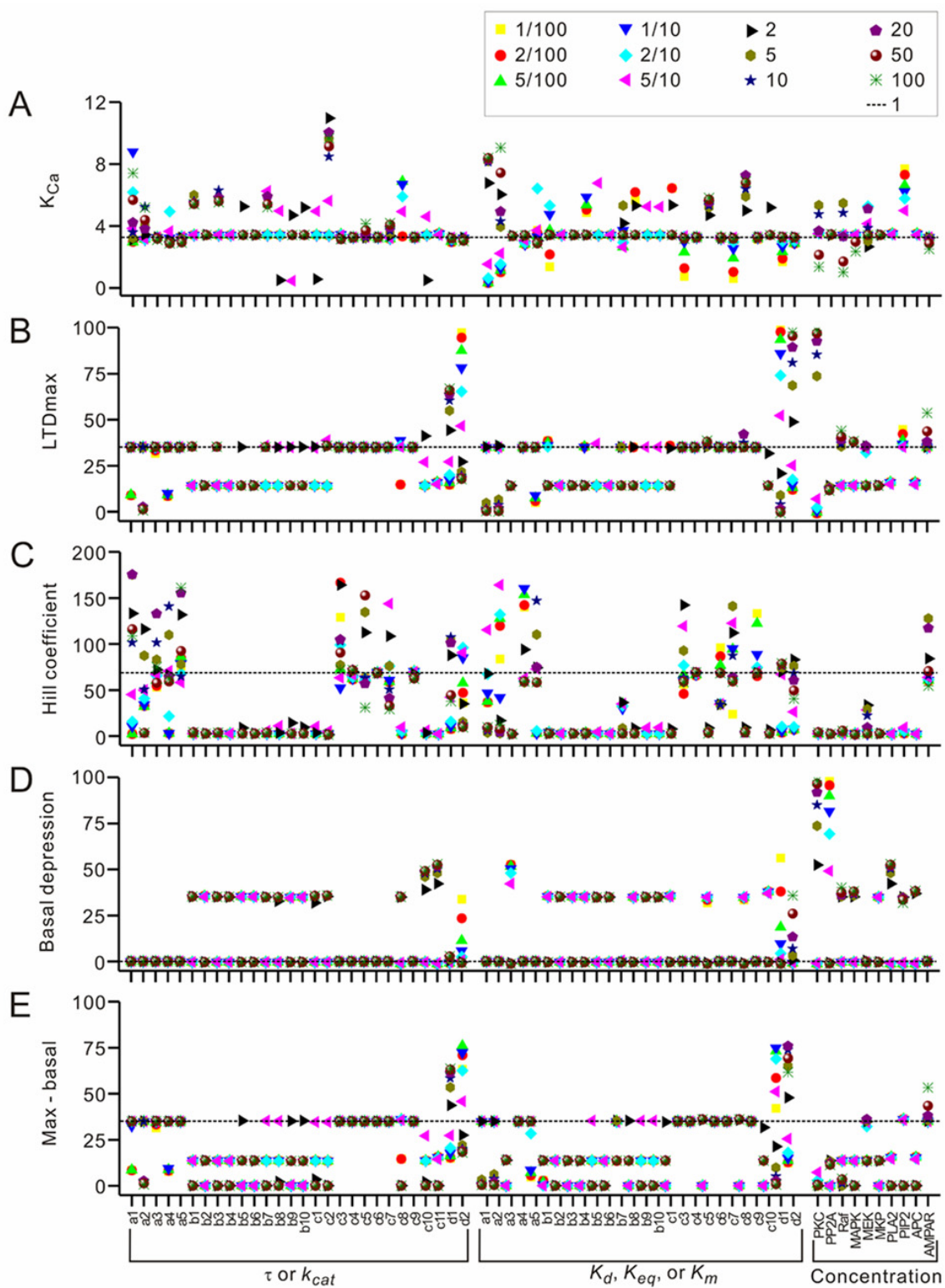


Figure S7

Parameter sensitivity analysis of the computational simulation

$K_{Ca}$  value (A), maximum amount of LTD (B), Hill coefficient (C), basal level of depression (D), and max-basal value (E), obtained in the parameter sensitivity analysis. Parameters varied in this analysis were time constant ( $\tau$ ),  $K_d$ , or  $K_{eq}$  in the biochemical reactions,  $k_{cat}$  or  $K_m$  in the enzymatic reactions, or concentrations of each reactant. Different symbols show different scaling factors that original parameter values were multiplied with (1/100 – 100).  $K_{Ca}$  value, maximum LTD, and Hill coefficient were determined only when the relationship could be described by Hill equation. Dashed lines show outcome produced by the parameter values used in the final model (Figure 7B). Note that the experimental conditions were not incorporated into these results.

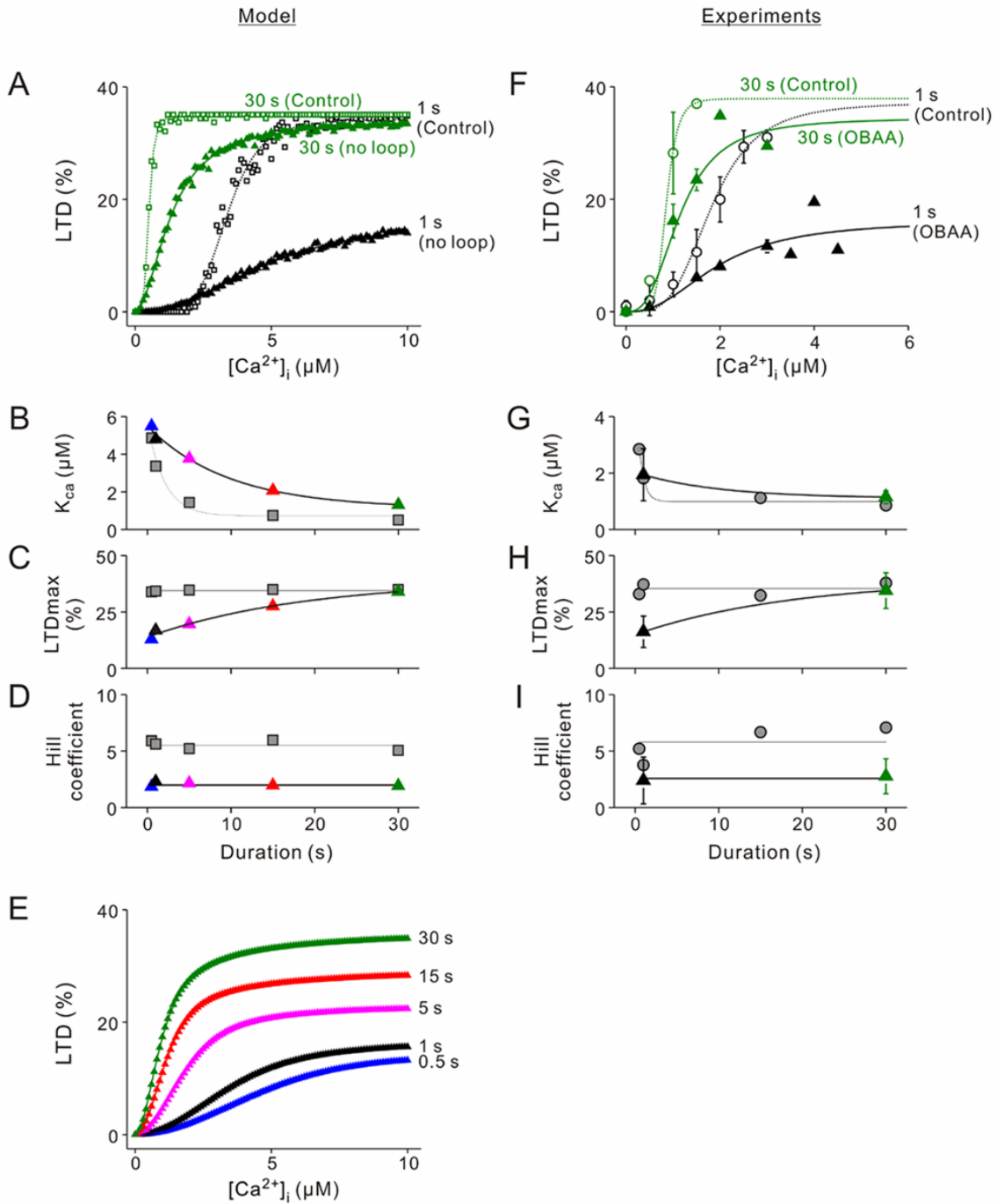


Figure S8

Cooperative triggering of LTD arises from the positive feedback loop

(A) Relationships between peak  $[Ca^{2+}]_i$  and LTD predicted by simulation in the absence of AA-mediated PKC activation (shown in Figure 9A) is superposed with

the control relationship (shown in Figure 7C). Relationships obtained by 1 s and 30 s duration of  $[Ca^{2+}]_i$  elevation are shown. (B-D)  $K_{Ca}$  value (B), maximum amount of LTD (C), and Hill coefficient (D) without the positive feedback loop are plotted against duration of  $[Ca^{2+}]_i$  elevation. These values were obtained from Hill equation used in Figure 9A. For comparison, control data shown in Figures 7D-F are also plotted as gray squares. (E) Simulated relationships between peak  $[Ca^{2+}]_i$  and LTD in the absence of activation of PKC by AA. These relationships were not corrected with the effects of non-uniform distribution of  $[Ca^{2+}]_i$  and noise. (F) Relationships between peak  $[Ca^{2+}]_i$  and LTD measured experimentally in the presence of PLA2 inhibitor, OBAA (shown in Figure 9F) is superposed with the control relationship (shown in Figure 5A). (G-I)  $K_{Ca}$  value (G), maximum amount of LTD (H), and Hill coefficient (I) are plotted against duration of UV pulse. These parameters were obtained from Hill equation used in Figure 9F. For comparison, control data shown in Figures 5B-5D are also plotted as gray circles.

Table S1

ID	Reaction name	Kinetic parameters			#Refs
a1	PKC_bind_Ca	$k_f = 0.25 \text{ s}^{-1} \mu\text{M}^{-2}$	$k_b = 1 \text{ s}^{-1}$	$K_d = 2 \mu\text{M}$	1
a2	PKC-Ca_memb	$k_f = 1 \text{ s}^{-1}$	$k_b = 0.1 \text{ s}^{-1}$	$K_{eq} = 10$	1
a3	PKC_bind_AA	$k_f = 0.2 \text{ s}^{-1} \mu\text{M}^{-1}$	$k_b = 10 \text{ s}^{-1}$	$K_d = 50 \mu\text{M}$	2
a4	PKC-AA_bind_Ca	$k_f = 0.25 \text{ s}^{-1} \mu\text{M}^{-2}$	$k_b = 1 \text{ s}^{-1}$	$K_d = 2 \mu\text{M}$	1
a5	PKC-Ca_bind_AA	$k_f = 0.2 \text{ s}^{-1} \mu\text{M}^{-1}$	$k_b = 10 \text{ s}^{-1}$	$K_d = 50 \mu\text{M}$	2
b1	PKC_phos_Raf	$K_m = 11.5 \mu\text{M}$	$k_{cat} = 0.0335 \text{ s}^{-1}$	$k_{-1}/k_{cat} = 4$	3, 4
b2	PP2A_deph_Raf-P	$K_m = 15.7 \mu\text{M}$	$k_{cat} = 6 \text{ s}^{-1}$	$k_{-1}/k_{cat} = 4$	5
b3	Raf_act_MEK	$K_m = 0.398 \mu\text{M}$	$k_{cat} = 0.105 \text{ s}^{-1}$	$k_{-1}/k_{cat} = 4$	6
b4	Raf_act_MEK-P	$K_m = 0.398 \mu\text{M}$	$k_{cat} = 0.105 \text{ s}^{-1}$	$k_{-1}/k_{cat} = 4$	6
b5	PP2A_deph_MEK-PP	$K_m = 15.7 \mu\text{M}$	$k_{cat} = 6 \text{ s}^{-1}$	$k_{-1}/k_{cat} = 4$	5, 7, 8
b6	PP2A_deph_MEK-P	$K_m = 15.7 \mu\text{M}$	$k_{cat} = 6 \text{ s}^{-1}$	$k_{-1}/k_{cat} = 4$	5, 7, 8
b7	MEK_act_MAPK	$K_m = 0.0463 \mu\text{M}$	$k_{cat} = 0.15 \text{ s}^{-1}$	$k_{-1}/k_{cat} = 4$	9, 10
b8	MEK_act_MAPK-P	$K_m = 0.0463 \mu\text{M}$	$k_{cat} = 0.15 \text{ s}^{-1}$	$k_{-1}/k_{cat} = 4$	9, 10
b9	MKP_deph_MAPK-PP	$K_m = 0.16667 \mu\text{M}$	$k_{cat} = 1 \text{ s}^{-1}$	$k_{-1}/k_{cat} = 4$	11, 12
b10	MKP_deph_MEPK-P	$K_m = 0.16667 \mu\text{M}$	$k_{cat} = 1 \text{ s}^{-1}$	$k_{-1}/k_{cat} = 4$	11, 12
c1	MAPK_phos_PLA2	$K_m = 25.6 \mu\text{M}$	$k_{cat} = 20 \text{ s}^{-1}$	$k_{-1}/k_{cat} = 4$	13, 14
c2	PLA2-P_deg	$k_f = 0.17 \text{ s}^{-1}$	$k_b = 0 \text{ s}^{-1}$		15
c3	PLA2_bind_Ca	$k_f = 0.01 \text{ s}^{-1}$	$k_b = 0.1 \text{ s}^{-1}$	$K_d = 10 \mu\text{M}$	16
c4	PLA2-PIP2_bind_Ca	$k_f = 0.01 \text{ s}^{-1}$	$k_b = 0.1 \text{ s}^{-1}$	$K_d = 10 \mu\text{M}$	16
c5	PLA2_bind_PIP2	$k_f = 0.0012 \text{ s}^{-1}$	$k_b = 0.48 \text{ s}^{-1}$	$K_d = 400 \mu\text{M}$	4
c6	PLA2-Ca_bind_PIP2	$k_f = 0.0012 \text{ s}^{-1}$	$k_b = 0.48 \text{ s}^{-1}$	$K_d = 400 \mu\text{M}$	4
c7	PLA2-Ca_prd_AA	$K_m = 20 \mu\text{M}$	$k_{cat} = 54 \text{ s}^{-1}$	$k_{-1}/k_{cat} = 4$	17
c8	PLA2-PIP2_prd_AA	$K_m = 20 \mu\text{M}$	$k_{cat} = 11.04 \text{ s}^{-1}$	$k_{-1}/k_{cat} = 4$	17
c9	PLA2-PIP2-Ca_prd_AA	$K_m = 20 \mu\text{M}$	$k_{cat} = 36 \text{ s}^{-1}$	$k_{-1}/k_{cat} = 4$	17
c10	PLA2-P_prd_AA	$K_m = 20 \mu\text{M}$	$k_{cat} = 120 \text{ s}^{-1}$	$k_{-1}/k_{cat} = 4$	17
c11	AA_deg	$k_f = 0.4 \text{ s}^{-1}$	$k_b = 0 \text{ s}^{-1}$		15
d1	PKC_phos_AMPAR	$K_m = 3.5 \mu\text{M}$	$k_{cat} = 0.05 \text{ s}^{-1}$	$k_{-1}/k_{cat} = 4$	4
d2	PP2A_deph_AMPAR-P	$K_m = 15.7 \mu\text{M}$	$k_{cat} = 6 \text{ s}^{-1}$	$k_{-1}/k_{cat} = 4$	5

$k_f$  and  $k_b$  are defined by formula S8.  
 $k_1$ ,  $k_{-1}$ , and  $k_{cat}$  are defined by formula S9.  
 $K_d$ : dissociation constant ( $K_d = k_b/k_f$ )  
 $K_{eq}$ : equilibrium constant ( $K_{eq} = k_b/k_f$ )  
 $K_m$ : Michaelis constant ( $K_m = (k_{-1} + k_{cat})/k_1$ )

#References are shown below Table S2.

Table S2

Molecular name	Full name	Concentration	#Refs
PKC	Protein kinase C	1 $\mu$ M	18
PP2A	Protein phosphatase 2A	0.045 $\mu$ M	19
Raf	Raf	0.5 $\mu$ M	20
MEK	MAPK or ERK kinase	0.5 $\mu$ M	9, 21
MAPK	Mitogen-activated protein kinase	1 $\mu$ M	13, 21
MKP	MAPK phosphatase	0.0032 $\mu$ M	22
PLA2	Phospholipase A2	0.4 $\mu$ M	16
PIP2	Phosphatidylinositol bisphosphate	10 $\mu$ M	4
APC	Arachidonylphosphatidylcholine	30 $\mu$ M	23
AMPA	AMPA receptor	0.5 $\mu$ M	24

## #References:

(1) Oancea and Meyer, 1998; (2) Schaechter and Benowitz, 1993; (3) Chen et al., 1993; (4) Kuroda et al., 2001; (5) Pato et al., 1993; (6) Force et al., 1994; (7) Kyriakis et al., 1992; (8) Ahn et al., 1999; (9) Seger et al., 1992; (10) Haystead et al., 1992; (11) Charles et al., 1992; (12) Charles et al., 1993; (13) Sanghera et al., 1990; (14) Nemenoff et al., 1993; (15) Bhalla and Iyengar, 1999; (16) Leslie and Channon, 1990; (17) Channon and Leslie, 1990; (18) Marquez et al., 1992; (19) Mumby et al., 1985; (20) Storm et al., 1990; (21) Huang and Ferrell, 1996; (22) Sun et al., 1993; (23) Wijkander and Sundler, 1991; (24) Tanaka et al., 2005

Table S3

ID	Sensitivities (standard deviation)									
	$\tau$ or $k_{cat}$					$K_d$ , $K_{eq}$ , or $K_m$				
	max-basal	basal	$K_{Ca}$	LTD max	Hill coef.	max-basal	basal	$K_{Ca}$	LTD max	Hill coef.
a1	11.55	0	1.93	11.46	65.52	17.12	0	3.76	16.95	33.41
a2	14.66	0	0.77	14.67	33.07	16.55	0	2.64	16.57	58.83
a3	1.02	0	0.05	1.01	22.00	10.47	26.35	0.04	7.93	25.08
a4	12.69	0	0.55	12.52	43.68	0.02	0	0.26	0.02	42.03
a5	0.02	0	0.14	0.02	34.19	13.46	0	0.94	13.58	46.43
b1	10.35	18.43	1.14	10.99	18.94	9.81	18.49	1.02	11.81	18.93
b2	10.39	18.54	0.06	7.87	25.01	10.39	18.40	0.06	7.86	25.01
b3	10.38	18.39	1.24	10.93	19.86	10.39	18.40	0.06	7.87	25.01
b4	10.38	18.36	0.06	7.87	25.01	10.36	18.38	0.99	10.95	19.85
b5	12.67	18.44	0.70	10.17	24.72	12.68	18.25	1.28	10.61	24.91
b6	10.38	18.44	0.06	7.87	25.01	10.39	18.29	0.06	7.87	25.01
b7	12.66	18.30	1.22	11.04	20.74	11.09	0.27	0.69	10.81	21.06
b8	12.52	18.13	1.24	10.77	23.12	12.67	18.30	1.19	10.97	21.87
b9	12.63	18.26	1.20	10.77	23.15	12.67	18.31	0.71	10.18	24.72
b10	12.66	18.29	0.68	10.18	24.71	12.67	18.30	0.70	10.18	24.72
c1	12.36	18.31	1.21	10.72	23.12	12.55	18.64	1.38	11.08	21.89
c2	12.53	18.65	3.20	11.14	18.43					
c3	0.04	0	0.14	0.03	36.51	0.16	0	0.85	0.09	27.75
c4	0.02	0	0	0.01	4.29	0.02	0	0	0.01	1.31
c5	0.02	0.02	0.26	0.04	34.82	18.64	18.17	0.88	1.38	2.13
c6	0.02	0	0	0.01	0.30	0.02	0	0.03	0.02	22.97
c7	0.02	0	0.37	0.05	31.01	0.08	0	0.91	0.04	31.87
c8	17.08	18.64	1.63	10.45	24.40	18.63	18.43	1.39	2.59	24.20
c9	0.02	0	0	0.01	3.26	0.02	0	0.04	0.02	22.29
c10	11.36	24.47	1.17	11.10	23.21	12.13	19.72	0.68	9.38	24.80
c11	10.82	26.39	0.09	7.31	25.10					
d1	20.13	1.50	0.12	21.56	39.66	29.06	18.10	0.58	41.07	34.89
d2	23.47	10.98	0.09	31.85	32.64	25.75	11.89	0.18	34.71	29.84

$\tau$ ; time constant of biochemical reactions.  
To multiply  $\tau$  with  $x$ , both  $k_f$  and  $k_b$  was divided by  $x$ .

Table S4

Molecular name	Sensitivities (standard deviation)				
	max-basal	basal	$K_{Ca}$	LTDmax	Hill coef.
PKC	9.60	44.94	1.02	44.38	18.92
PP2A	10.16	43.85	0.07	8.51	25.09
Raf	9.61	19.20	1.16	12.94	18.83
MEK	10.38	19.28	0.36	11.48	22.12
MAPK	11.05	0.27	0.76	10.76	19.75
MKP	10.39	18.32	0.06	7.87	25.01
PLA2	10.82	26.38	0.09	7.30	25.10
PIP2	18.64	18.17	1.50	3.82	24.27
APC	10.75	20.15	0.09	7.36	25.10
AMPA	5.33	0.10	0.22	5.43	22.96